NJC

New Journal of Chemistry

A journal for new directions in chemistry

Accepted Manuscript

This article can be cited before page numbers have been issued, to do this please use: S. Rayati, D. Moradi and F. Nejabat, *New J. Chem.*, 2020, DOI: 10.1039/D0NJ04190D.

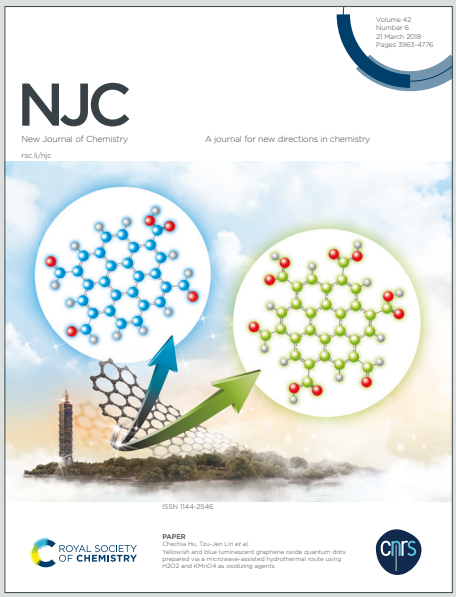

ROYAL SOCIETY OF CHEMISTRY

rsc.li/njc

View Article Online
DOI: 10.1039/D0NJ04190D

Journal Name

ARTICLE

Magnetically recoverable porphyrin-based nanocatalyst for the effective oxidation of olefins with hydrogen peroxide: a comparative study

Saeed Rayati*, Dana Moradi and Fatemeh Nejabat

Abstract

In this paper, preparation, characterization and catalytic application of metalloporphyrin-based magnetic nanocatalysts were investigated. *meso*-tetrakis(4-carboxyphenyl) porphyrinatoiron (III) chloride (Fe(TCPP)Cl) and *meso*-tetrakis(4-carboxyphenyl) porphyrinatomanganese (III) acetate (Mn(TCPP)OAc) were separately immobilized of onto the surface of amine functionalized magnetic nanoparticles ($Fe_3O_4/SiO_2/NH_2$) via covalent attachment. The obtained nanocatalysts were characterized by FT-IR and UV-Vis and atomic absorption spectroscopy, X-ray powder diffraction (XRD), vibrating sample magnetometry (VSM), thermogravimetric analysis (TGA), transmission electron microscope (TEM). The catalytic efficiency of $Fe_3O_4/SiO_2/NH_2$-Fe(TCPP)Cl and $Fe_3O_4/SiO_2/NH_2$-Mn(TCPP)OAc for the green oxidation of alkenes with H_2O_2 were investigated in a comparative manner. Mn-porphyrin based magnetic nanocatalyst shows higher catalytic efficiency compared to the Fe--porphyrin. In addition, the prepared magnetic nanocatalyst exhibited excellent reusability and could be reused at least for five times without significant leaching or loss of activity.

Introduction

Oxidation of olefins is one of the great interests of the pharmaceutical and industrial chemistry due to the importance of valuable oxygen containing products.[1-3] To achieve unique products with excellent yield and selectivity, oxidation of olefins were conducted over various metal complexes as catalysts in homogeneous and heterogeneous systems and many scientists were greatly focused on designing effective catalysts for oxidation reactions.[4-7] Cytochrome P450 plays an important role in oxidation reactions of metabolic processes and participate in various oxygenations.[8] Metalloporphyrins can be an ideal biomimetic model of CY-P450 to study details of biological systems and to improve the development of synthetic catalysts.[9-14] Although the catalytic reactions in the homogeneous systems exhibit high activity (because of its large surface area), but these kind of catalysts have many disadvantages such as economic drawbacks regard to the difficulties of the separation and the contamination of the products.[15-18] Recently, a great deal of effort was devoted to the application of nanomaterials i.e. nanosheets,[19-21] nanotubes[22-24] and nanoparticles [25-27] as support for the preparation of various effective heterogenized catalyst. Apart from the well-known organic and inorganic support, functionalized magnetic nanoparticles because of their chemical, structural and high magnetic properties could get more attention as valuable materials for the attachment of metal complexes to prepare reusable nanocatalyst.[28-32]

By considering and discussing the environmental issues, many attempts were focused on the applying of the principles of green chemistry in the catalytic reactions.[33-34] Recently, employing hydrogen peroxide as a biodegradable, cheap, safe and green oxidant for the catalytic oxidation reactions is an ideal method for the development of green chemistry in the chemical synthesis.[34-37] In this study, in continuing our studies about preparation of porphyrin based nanocatalysts and comparing the effect of metal center on the catalytic efficiency of nanocatalysts, Mn and Fe porphyrins immobilized onto the surface of amine functionalized magnetic nanoparticles as efficient catalysts for the oxidation of olefins with H_2O_2.

Experimental

Chemicals and Instruments.

Chemical reagents and solvents were purchased from Merck, Aldrich, Scharlau or Fluka and used without further purification.

UV-Vis spectra were recorded with a Lambda 25 Perkin Elmer spectrophotometer from 400-700 nm. Fourier transform infrared (FT-IR) spectra were recorded (KBr pallets) on an ABB Bomem: FTLA 2000-100 in the range of 400-4000 cm^{-1}. Manganese and iron content were determined by using a Varian AA240 atomic absorption

[a]Department of Chemistry, K.N. Toosi University of Technology, P.O. Box 16315-1618, Tehran 15418, Iran. E-mail: rayati@kntu.ac.ir
Fax: +98 21 22853650; Tel: +98 21 22850266

spectrometer. The morphology features of solid samples were investigated by transmission electron microscopy (TEM; Zeiss-EM10C-100 KV). The crystalline structure of obtained samples was identified by X-ray powder diffraction (XRD) using a Panalytical Xpert PRO X Ray Diffractometer (Xpert Pro MPD) with Cu-kα radiation (λ=0.15418) at 40kV and 40mA. Thermal stability of samples was investigated by the thermal gravimetric analysis (Mettler-Toledo TGA 851e). Magnetic properties of materials determined on a BHV-55 vibrating sample magnetometer (VSM) at room temperature. Purity determinations of the products were accomplished by GC-FID on an Agilent 7890B instrument using a SAB-5 capillary column (phenyl methyl siloxane 30m × 0.32 mm × 0.25 µm).

Synthesis of nanocatalyst [$Fe_3O_4/SiO_2/NH_2$-M(TCPP)]

Porphyrins and metalloporphyrins were synthesized by using Adler's method (See Supporting information).[38,39] Silica coated magnetic nanoparticles (Fe_3O_4/SiO_2) was prepared and functionalized with 3-aminopropyltriethoxysilane (APTS) as reported previously (See Supporting information).[40-44] Metalloporphyrins (Fe(TCPP)Cl or Mn(TCPP)OAc) were covalently attached to the surface of $Fe_3O_4/SiO_2/NH_2$ to prepare magnetic nanocatalysts in the presence of TBTU/DIPEA.[37,38] In brief, metalloporphyrin (0.6 g of Fe(TCPP)Cl or Mn(TCPP)OAc) was dissolved in DMF (40 mL), 2-(1H-benzotriazole-1-yl)-1,1,3,3-tetramethyluronium tetrafluoroborate (TBTU) (0.4 g), (N,N'-diisopropylamine) (DIPEA) (0.3 g) and $Fe_3O_4/SiO_2/NH_2$ (1 g) were added to the solution and the mixture was stirred for about 48 h at room temperature. The supported magnetic nanocatalyst was collected by a magnet, washed several times with DMF and ethanol and dried at 50 °C for about 20 hours.

General procedure for alkene oxidation

Oxidation reaction of olefins in the presence of $Fe_3O_4/SiO_2/NH_2$-M(TCPP) (M: Fe or Mn) as catalyst is elaborated as follows: In a test tube, 0.0025 mmol of the prepared nanocatalyst (0.005 g), 0.2 mmol of substrate, 0.12 mmol of imidazole (ImH) and 0.7 mL H_2O_2 as an oxidant were added in 1 mL acetonitrile. The reaction was stirred at room temperature for an appropriate time and at the end of the oxidation reaction, the heterogenized catalyst was separated from the reaction media by a magnet and gas chromatography was used to analyze the reaction progress.

Results and discussion

Preparation of nanocatalyst

The heterogenized nanocatalysts $Fe_3O_4/SiO_2/NH_2$@M(TCPP) (M is manganese or iron) were prepared as illustrated in Scheme 1.

Fe_3O_4 nanoparticles synthesized via precipitation method, coated by silica and functionalized by amine groups as reported previously.[43] The "one pot" amidic reaction of carboxylic groups of metalloporphyrins and amine groups of magnetic supports was carried out using TBTU as a coupling reagent and DIPEA as a base in DMF at room temperature. TBTU is an uronium salt commonly used in amidation and esterification reactions, especially in basic solutions.[24,44]

Characterization of the catalyst $Fe_3O_4/SiO_2/NH_2$-MTCPP

The amount of attached metalloporphyrins onto the surface of $Fe_3O_4/SiO_2/NH_2$ was determined by UV-Vis and atomic absorption spectroscopy (AAS). Based on the results, each gram of $Fe_3O_4/SiO_2/NH_2$-FeTCPP(Cl) and $Fe_3O_4/SiO_2/NH_2$-MnTCPP(OAc) contain 500 and 520 µmol of metalloporphyrin respectively.

The FT-IR spectra of the synthesized nanomaterials are presented in Figure 1. The strong absorption bands at 468 cm^{-1}, 586 cm^{-1} and 669 cm^{-1} are related to stretching vibration of Fe-O in Fe_3O_4, which could be detectable in all samples (Figure 1).

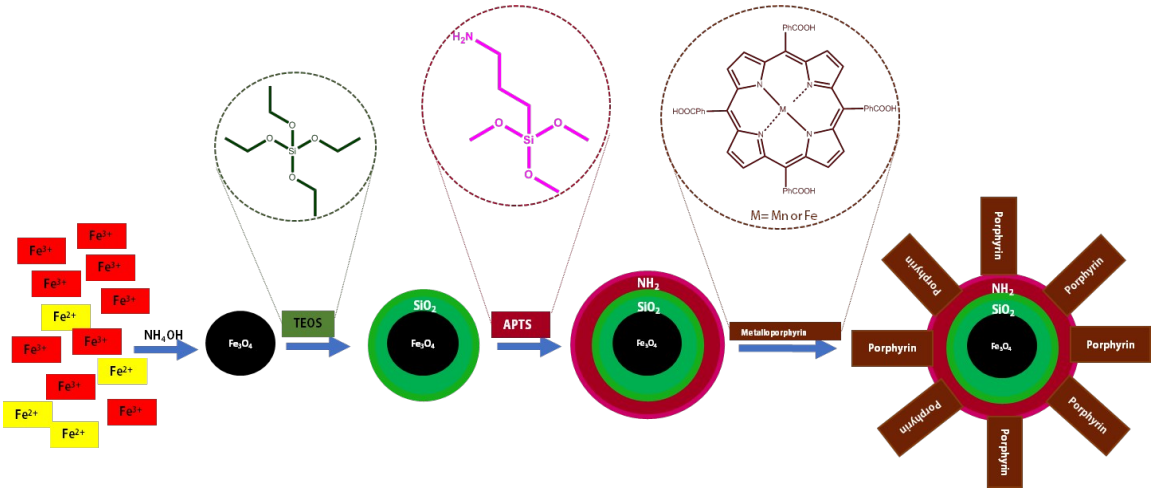

Scheme 1. Schematic preparation of magnetic nanocatalyst.

View Article Online
DOI: 10.1039/D0NJ04190D

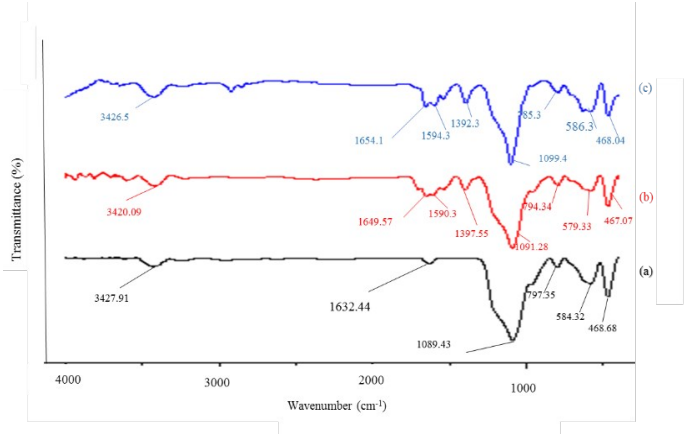

Figure 1. FTIR spectra of (a) $Fe_3O_4/SiO_2/NH_2$, (b) $Fe_3O_4/SiO_2/NH_2$-FeTCPP(Cl) and (c) $Fe_3O_4/SiO_2/NH_2$-MnTCPP(OAc).

The strong absorption bands at 1090 cm^{-1} and 790 cm^{-1} are assigned to anti-symmetric stretching of O-Si-O and symmetric stretching of this band, which reveal that the Fe_3O_4/SiO_2 has been successfully prepared. In addition, the peaks at 1630 cm^{-1} and 3420 cm^{-1} can be attributed to amino functionalizing of Fe_3O_4/SiO_2. After metalloporphyrin immobilization, a new absorption band could be detectable around 1650 cm^{-1}, which evidently indicates the formation of amide bond between carboxyl groups (-COOH) of metalloporphyrins and amine groups (-NH_2) of the magnetic support (Figure 1, b and c). Moreover, the absorption band at 1397 cm^{-1} is attributed to the vibrations of metalloporphyrin .[43,45]

To investigate the crystalline structure and phase purity of nanomaterials, (XRD) patterns of $Fe_3O_4/SiO_2/NH_2$-FeTCPP(Cl) and $Fe_3O_4/SiO_2/NH_2$-MnTCPP(OAc) were recorded and presented in Figure 2. Based on the results, the main peaks 2θ values of 31, 36, 43, 53, 57 and 63 deg. corresponding to (220), (311), (400), (422), (511) and (440) plans of cubic inverse spinel Fe_3O_4 [39,41] are similar in the pattern of the prepared magnetic nanocatalysts and solid supports (Figure SI) with similar lattice constant (Table SI). The observed diffraction peaks are in good agreement with database of JCPDS file (Ref. Code 96-900-2322) and revealed the stability of crystalline structure of magnetic nanoparticles during the subsequent modification.

Moreover, based on Debye–Scherrer equation ($D = 0.9\lambda/B \cos\theta$), the average crystallite size of $Fe_3O_4/SiO_2/NH_2$, $Fe_3O_4/SiO_2/NH_2$-Mn(TCPP)OAc and $Fe_3O_4/SiO_2/NH_2$-Fe(TCPP)Cl were calculated to be 18, 21 and 28 nm, respectively. Based on the results after porphyrin deposition, the average particle sizes of magnetic nanoparticles were increased and less crystallinity was observed; which can be attributed to the attachment of metalloporphyrins onto the surface of $Fe_3O_4/SiO_2/NH_2$.

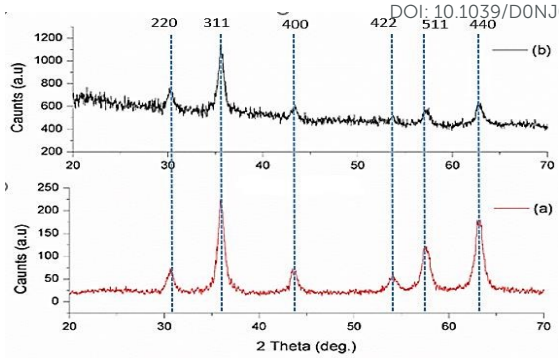

Figure 2. XRD pattern of (a) $Fe_3O_4/SiO_2/NH_2$-Mn(TCPP)OAc and (b) $Fe_3O_4/SiO_2/NH_2$-Fe(TCPP)Cl.

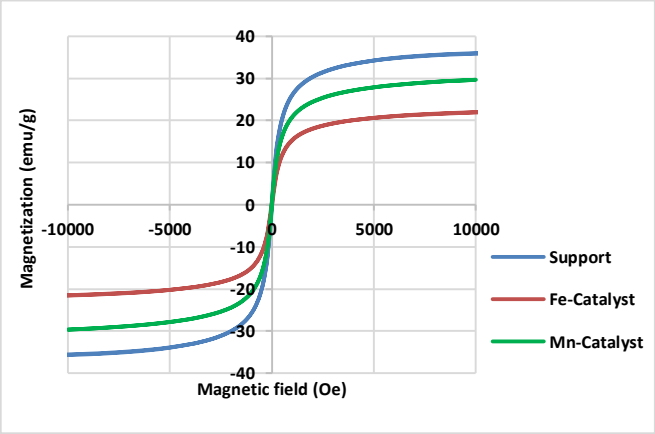

Figure 3. Magnetization curve of $Fe_3O_4/SiO_2/NH_2$, $Fe_3O_4/SiO_2/NH_2$-Mn(TCPP)OAc and $Fe_3O_4/SiO_2/NH_2$-Fe(TCPP)Cl.

The magnetic characteristics of $Fe_3O_4/SiO_2/NH_2$ and the nanocatalysts were evaluated by vibrating sample magnetometer (VSM), which illustrates ferromagnetic behaviour of the prepared samples (Figure 3). The prepared nanomaterials are superparamagnetic and no coercivity (H_C) and remanent magnetization (M_R) were observed in the curves (Figure 3). The saturated magnetization values of $Fe_3O_4/SiO_2/NH_2$, $Fe_3O_4/SiO_2/NH_2$-Fe(TCPP)Cl and $Fe_3O_4/SiO_2/NH_2$-Mn(TCPP)OAc are 36, 22 and 20 amu/g respectively. Although because of diamagnetic behavior of the surface, the magnetization of the nanocatalysts is diminished compared to the Fe3O4, but the prepared nanocatalysts still respond sufficiently to the external magnetic field.[46-48]

To study thermal stability of magnetic nanocatalysts, thermo-gravimetric analysis (TGA) of $Fe_3O_4/SiO_2/NH_2$-Fe(TCPP)Cl and $Fe_3O_4/SiO_2/NH_2$-Mn(TCPP)OAc were investigated under O_2 atmosphere (100 mL/min) at the heating rate of 10 °C/min in the range between room temperature and 800 °C (Figure 4). The thermal behaviour of magnetic nanocatalysts show a weight loss at about 130 °C, which is due to the loss of physically adsorbed water molecules. The next weight loss between 170 °C and 280 °C could be attributed to desorption of water molecules; which have chemical bond with SiO_2. In the TGA curves of nanocatalysts, the weight loss between 320

View Article Online
DOI: 10.1039/D0NJ04190D

°C and 800 °C could be related to decomposition of organic parts, metalloporphyrin and formation of metal oxide.[49-50]

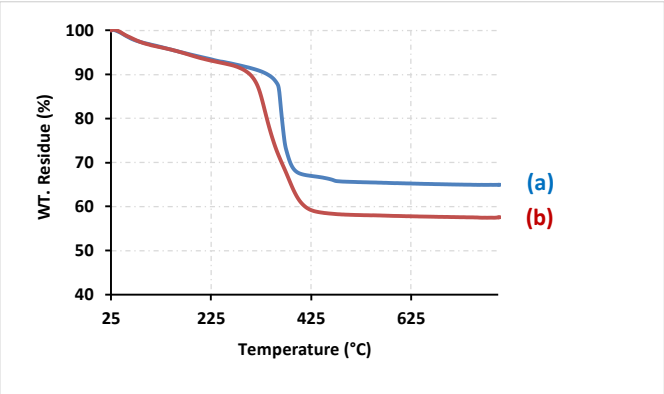

Figure 4. TGA Diagram of (a) $Fe_3O_4/SiO_2/NH_2$-Mn(TCPP)OAc and (b) $Fe_3O_4/SiO_2/NH_2$-Fe(TCPP)Cl.

Figure 5 shows the UV-Vis spectra of dispersed $Fe_3O_4/SiO_2/NH_2$, $Fe_3O_4/SiO_2/NH_2$-Fe(TCPP)Cl and $Fe_3O_4/SiO_2/NH_2$-Mn(TCPP)OAc in ethanol. The UV-Vis spectra of magnetic nanocatalyst displayed the typical Soret band of metalloporphyrins (420 nm for iron porphyrins and 470 nm for manganese porphyrins respectively) and there is no detectable peak in this region in the UV-Vis spectrum of $Fe_3O_4/SiO_2/NH_2$ (Figure 5, c). These data indicated metalloporphyrins successfully immobilized onto the surface of Fe3O4@SiO_2NH_2 without any distortion or aggregation.

The morphology of original $Fe_3O_4/SiO_2/NH_2$, $Fe_3O_4/SiO_2/NH_2$-Fe(TCPP)Cl and $Fe_3O_4/SiO_2/NH_2$-Mn(TCPP)OAc were characterized by transmission electron microscope (TEM) which are shown in Figure 6. The TEM images show uniformity and homogeneous spherical morphology of all three samples with little aggregation. The core/shell nanostructures of magnetic nanomaterials clearly are detectable in the TEM images and shows that the core of Fe_3O_4 totally covered by silica layer and organic materials (Figure 6, (b)).

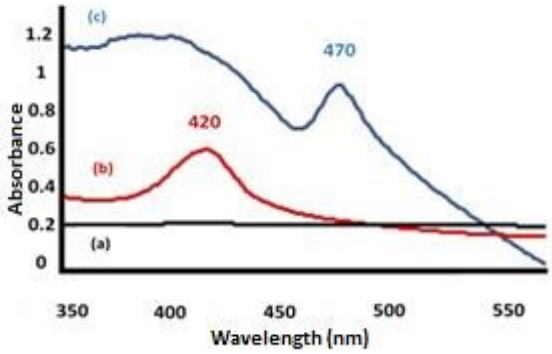

Figure 5. UV-Vis spectra of (a) $Fe_3O_4/SiO_2/NH_2$, (b) $Fe_3O_4/SiO_2/NH_2$-Fe(TCPP)Cl and (c) $Fe_3O_4/SiO_2/NH_2$-Mn(TCPP)OAc

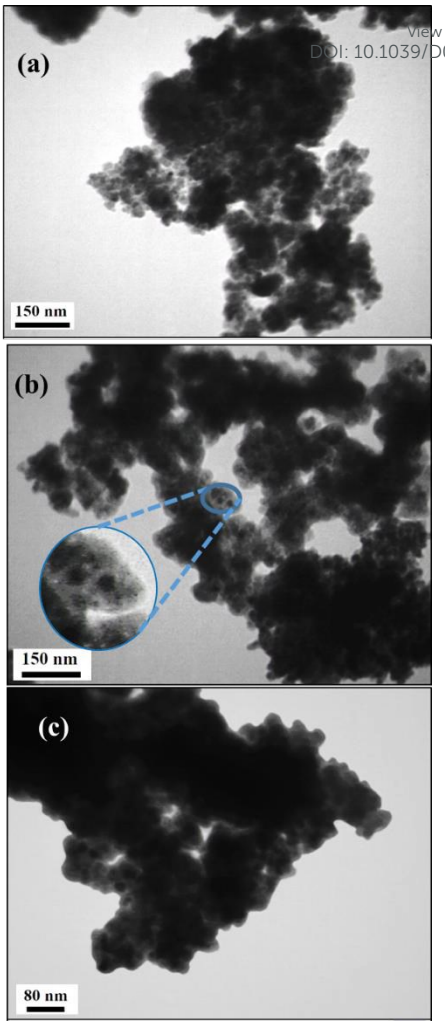

Figure 6. TEM image of (a) $Fe_3O_4/SiO_2/NH_2$, (b) $Fe_3O_4/SiO_2/NH_2$-Mn(TCPP)OAc and (c) $Fe_3O_4/SiO_2/NH_2$-Fe(TCPP)Cl.

Catalytic activity of magnetic nanocatalysts

The catalytic properties of two magnetic nanocatalysts was investigated for the green oxidation of olefins with H_2O_2 and the effect of metal centre of metalloporphyrins on the catalytic efficiency of the prepared nanocatalysts were compared. The oxidation of cyclooctene with hydrogen peroxide was used as a model reaction; to achieve the best reaction condition, different parameters such as solvent, reaction time, temperature, amount of imidazole and the amount of H_2O_2 were studied and the catalytic efficiency of Mn-catalyst and Fe-catalyst were compared in all cases.

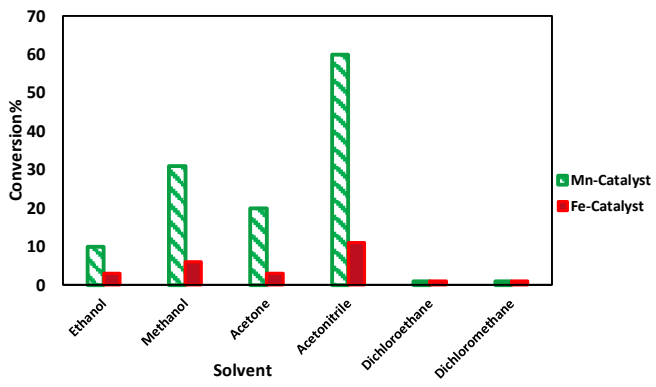

Figure7. The effect of solvent on the oxidation of cyclooctene with H_2O_2 in the presence of magnetic nanocatalysts. The molar ratio of Catalyst:Cyclooctene:ImH is (1:80:50), H_2O_2(1 mL), r.t, Time: 5 h

In order to investigate the effect of solvent on the catalytic oxidation of cyclooctene with H_2O_2 in the present of magnetic nanocatalysts, different solvents such as ethanol, methanol, acetone, dichloromethane, dichloroethane and acetonitrile were applied and the results are presented in Figure 7. Based on the results, the highest conversion was obtained in acetonitrile (60%), no significant product was obtained in dichloroethane and dichloromethane (1%), since aqueous hydrogen peroxide is insoluble in organic solvents and two-phase system were obtained in these solvents. It should be noted that epoxy cyclooctane was the sole product of this oxidation reaction and the reaction did not proceed in the absence of the catalyst.

To achieve the best amount of oxidant for the green oxidation of cycloocetene, different amount of H_2O_2 were utilized while other parameters were maintained constant for the oxidation reaction in CH_3CN (Table 1). Hydrogen peroxide is an inactive oxidant for the epoxidation reaction at room temperature; no significant amount of the products was detectable for the oxidation reaction in presence of three equivalent of the oxidant (Table 1, entry 1) and excess amount of H_2O_2 was required to achieve the acceptable results (Table 1, entry 2-4).

Table 1. Optimization of the amount of oxidant on the oxidation of cyclooctene with H_2O_2 in the presence of magnetic nanocatalysts.

Entry	H_2O_2 (mL)	Conversion %[a]	
		Mn-catalyst	Fe-catalyst
1	0.061	1	2
2	0.4	20	7
3	0.7	95	15
4	1	60	11

[a] Reaction condition: The molar ratio of catalyst: cyclooctene: ImH is (1:80:50), CH_3CN: 1 mL, Time: 5 h, temperature: 25 °C.

The highest conversion was obtained by addition of 0.7 mL of H_2O_2, but the conversion was decreased by increasing the amount of H_2O_2 up to 1 mL, which could be due to decomposition of nanocatalyst in the presence of higher amount of the oxidant (Table 1, entry 3-4)

Green oxidation of cyclooctene with H_2O_2 in the present of magnetic nanocatalysts was carried out in different times and the results are presented in Figure 8. After three hours acceptable conversion was obtained in the presence of Mn-catalyst (80%), while very little amount of epoxy cyclooctane was achieved in the presence of Fe-catalyst (9%) (Figure 8). By continuing the reaction for up to 10 hours, the oxidation reaction almost completed in the presence of $Fe_3O_4/SiO_2/NH_2$-Mn(TCPP)OAc, but the kinetics of the catalytic oxidation reaction with H_2O_2 in the presence of $Fe_3O_4/SiO_2/NH_2$-Fe(TCPP)Cl was slow and only 44% of epoxy cyclooctene was achieved after 24 hours. However, after 48 hours the oxidation reaction completed in the presence of $Fe_3O_4/SiO_2/NH_2$-Fe(TCPP)Cl.

According to the literature, presence of a nitrogenous base as an axial base increases the catalytic efficiency of metalloporphyrins for the oxidation reaction.[51] Oxidation of cyclooctene with H_2O_2 in the presence of magnetic nanocatalysts in different amount of imidazole was studied and the results are presented in Table 2.

The obtained results reveal that optimal ratio of catalyst:ImH is 1:50 and more amount of ImH inhibited the reaction significantly, which could be due to the formation of inactive six coordinate species, i.e. $M(por)(ImH)_2$.[52]

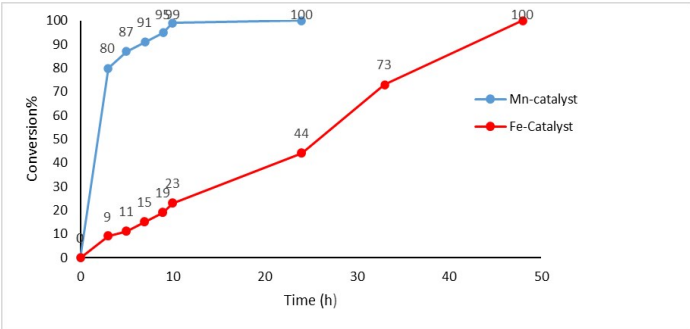

Figure 8. Optimization of time on the oxidation of cyclooctene with H_2O_2 in the presence of magnetic nanocataltsyts. Reaction condition: The molar ratio of Catalyst:Cyclooctene:ImH is (1:80:50), H_2O_2: 0.7 mL, CH_3CN: 1 mL, r.t.

View Article Online
DOI: 10.1039/D0NJ04190D

Table 2. Optimization of amount of ImH on the oxidation of cyclooctene with H_2O_2 in the presence of magnetic nanocatalysts at room temperature.

Entry	ImH:Catalyst	Conversion%[a]	
		Mn-catalyst	Fe-catalyst
1	5	1	2
2	25	14	5
3	50	92	11
4	75	78	8
5	100	73	7

[a] Reaction conditions: The molar ratio of Catalyst:Cyclooctene:ImH is (1:80:X), H_2O_2: 0.7 mL, CH_3CN: 1 mL, Time: 5 h.

The effect of reaction temperature on the oxidation of cyclooctene with H_2O_2 in acetonitrile in the presence of magnetic nanocatalysts were investigated (Table 3). The results illuminate that low temperature has a negative effect on the kinetic of the oxidation reactions and low amount of epoxy cyclooctane was achieved in the presence of both Fe and Mn nanocatalysts at 5 °C (Table 3). Based on the results, Mn-catalyst shows the best catalytic efficiency at room temperature and low amount of the product was obtained in higher or lower temperature. But on the contrary, the catalytic efficiency of $Fe_3O_4/SiO_2/NH_2$-Fe(TCPP)Cl increase by increasing the temperature and the best result was obtained at reflux (Table 3).

To generalize the applicability of the prepared magnetic nanocatalysts for the oxidation of olefins with hydrogen peroxide, oxidation of various olefins was carried out under the optimum reaction condition in the presence of both Fe-catalyst and Mn-catalyst and the results are presented in Table 4. Excellent results were obtained for the oxidation reaction with H_2O_2 in the presence of both Fe-catalyst and Mn-catalyst for all the olefins.

Table 3. Effect of temperature on oxidation of cyclooctene with H_2O_2 in the presence of magnetic nanocatalysts.

Entry	Temperature (℃)	Time (h)	Conversion %[a]	
			Mn-Catalyst	Fe-Catalyst
1	5	3	3	1
		5	3	1
2	25	3	85	4
		5	87	15
3	45[b]	3	36	30
		5	37	32
4	Reflux[b]	3	34	74
		5	36	97

[a] Reaction condition: Catalyst:cyclooctene:ImH (1:80:50). CH_3CN: 1 mL, H_2O_2: 0.7 mL. [b] Based on , 0.005 mmol of the catalyst, CH_3CN: 2 mL, H_2O_2: 1.4 mL.

Table 4. Oxidation of various olefins with H_2O_2 in the presence of magnetic nanocatalysts at room temperature.

No.	Alkene	Time (h)	Conversion%[a] (Selectivity%[b])	
			Mn-Catalyst	Fe-Catalyst[(c)] [(c)]
1		3	85 (100)	74 (100)
		5	87 (100)	97 (100)
2		3	75 (93)	96 (73)
		5	89 (84)	100 (84)
3	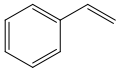	3	74 (78)	69 (87)[d]
4	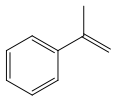	3	78 (64)	66 (97)[d]
		5	83 (50)	71 (94)[d]
5	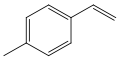	3	80 (47)	53 (94)[d]
		5	85 (33)	55 (94)[d]
6	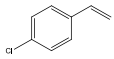	3	19 (63)	40 (82)[d]
		5	72 (92)	60 (78)[d]
7	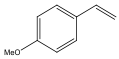	3	87 (57)	31 (100)
		5	99 (48)	67 (82)
8	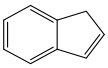	3	16 (75)	83 (31)
		5	86 (50)	90 (64)
9	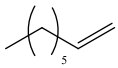	3	10 (100)	32 (100)
10		3	31 (100)	18 (100)
		5	39 (100)	22 (100)

[a] Reaction condition: Catalyst:substrate:ImH(1:80:50), Solvent:CH_3CN:1 mL, H_2O_2:0.7 mL, r.t. [b] Selectivity to the corresponding epoxide. [c] Based on 0.005 mmol of the catalyst, Reflux, CH_3CN: 2 mL, H_2O_2: 1.4 mL.. [d] Selectivity to the corresponding aldehyde.

The major product for the oxidation of olefins with H_2O_2 in the presence of Mn-catalyst was the corresponding epoxide, but the same result was not obtained in the presence of Fe-catalyst and in some cases, the corresponding aldehyde was the major product. The sole product of the oxidation of cyclooctene, 1-octene and *cis*-stilbene with H_2O_2 was their corresponding epoxide in the presence of both catalysts and for the oxidation of cyclohexene and indene, the corresponding epoxide was the major product. In the oxidation of styrene, α-methylstyrene, 4-methylstyrene, 4-chlorostyrene and 4-metoxystyrene the corresponding aldehyde were detected (by GC) as the major product in the oxidation reaction in the presence of Fe-

View Article Online
DOI: 10.1039/D0NJ04190D

catalyst, which indicates that ring-opening of epoxide can be proceeded under the reflux condition. Furthermore, it seems that the catalytic efficiency of $Fe_3O_4/SiO_2/NH_2$-Mn(TCPP)OAc for epoxidation with hydrogen peroxide is strongly dependent on the electronic property of substrates not the steric effects of the substrates (Table 4, Entry 3-7); but the catalytic efficiency of Fe-catalyst for the oxidation of various olefins does not follow a specific order. In addition, the lowest conversion was reached for the oxidation of 1-octene as a linear olefin due to the lack of electron density and conjugated π-bonding system.

To prove the catalytic efficiency of the supported nanocatalysts, oxidation of cyclooctene with H_2O_2 was carried out in the absence of catalyst, in the presence of unsupported metalloporphyrins and in the presence of supported nanocatalysts in the same condition (Table 5). Based on the results, no significant product was obtained after 5 hours in the absence of catalyst (1%), which indicate the critical role of the catalyst in the oxidation reaction (Table 5, entry 1). Although the reaction proceeded well in the presence of unsupported Mn(TCPP)OAc (conversion 75%); but only 8% of epoxy cyclooctane was obtained in the present of Fe(TCPP)Cl. By utilizing heterogeneous catalysts in the oxidation reaction, not only higher amount of epoxy cyclooctene were obtained, but also magnetic nanocatalysts were easily separated from the reaction media by an external magnet to use for the next run. It is clearly detectable that the rate of oxidation increases by the attachment of metalloporphyrin onto the surface of a magnetic nano-support.

The stability and reusability of magnetic nanocatalyst was investigated by recycling experiment for the oxidation of cyclooctene with H_2O_2 in the presence of $Fe_3O_4/SiO_2/NH_2$-Mn(TCPP)OAc in acetonitrile. After each catalytic cycle, the catalyst separated with an external magnet, washed with acetonitrile and acetone (2 mL, 2×2 time), dried at 60 °C and directly used in the next run.

Table 5. Oxidation of cyclooctene with H_2O_2 in the present of supported and unsupported catalysts at room temperature.

Entry	Catalyst	Conversion%[a]	TON
1	None	1	-
2	$Fe_3O_4/SiO_2/NH_2$	12	-
3	Fe(TCPP)Cl	8	6.4
4	Mn(TCPP)OAc	72	57.6
5	$Fe_3O_4/SiO_2/NH_2$-Mn(TCPP)OAc	87	69.6
6	$Fe_3O_4/SiO_2/NH_2$-Fe(TCPP)Cl	11	8.8

[a] Reaction condition: The molar ration of catalyst:cyclooctene:ImH is (1:80:50), Solvent:CH_3CN:1 mL, H_2O_2:0.7 mL, r.t, reaction time: 5 h.

Table 6. The result of reusability of $Fe_3O_4/SiO_2/NH_2$-MnTCPP(OAc) for oxidation of cyclooctene with H_2O_2.

Run	Conversion %[a]	Mn-leaching %[b]
1	87	0
2	64	0
3	60	0.8
4	60	0.3
5	58	3

[a]Reaction condition: The molar ration of catalyst:cyclooctene:ImH is (1:80:50), Solvent:CH_3CN:1 mL, H_2O_2:0.7 mL, 7 h, r.t.
[b] Mn-leaching was determined by AAS.

Based on the results, the prepared magnetic nanocatalyst showed excellent reusability in five consecutive cycles with a little loss of activity (Table 6).

To study the stability of magnetic nanocatalyst, after each catalytic reaction, Mn leaching of $Fe_3O_4/SiO_2/NH_2$-Mn(TCPP)OAc was evaluated by AAS and the results showed little amount of manganese in the filtrate; which reveals the stability of the prepared magnetic nanocatalyst (Table 6). Moreover, the XDR pattern of the used catalyst indicated that magnetic nanocatalyst is quite stable and no significant change was identified in the XRD pattern of Fe_3O_4/SiO_2/NH-Mn(TCPP)OAc (Figure 9).

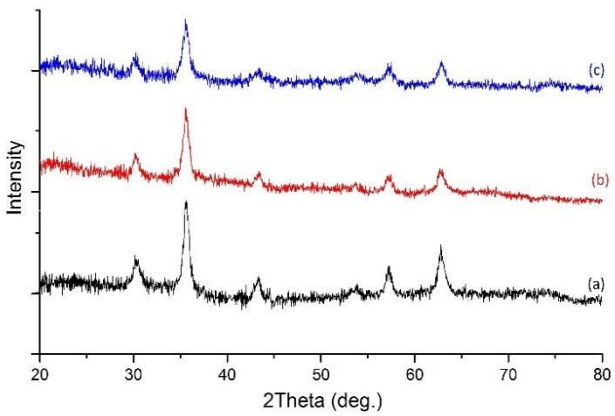

Figure 9. XRD pattern of (a) amine functionalized magnetic support, (b) fresh catalyst and (c) reused catalyst.

According to the literature, a possible mechanism was proposed for the oxidation of olefins with hydrogen peroxide (Scheme SI). In the catalytic cycle of metalloporphyrins for epoxidation with H_2O_2, two common intermediate have been suggested (a six-coordinate active species and a high valent metal-oxo (M=O)), which are responsible for oxygen transfer in a parallel process (Scheme SI, (a) and (b)).

To evaluate the catalytic efficiency of the prepared nanocatalysts, the catalytic results were compared with the previous reported data for epoxidation of cyclooctene in the presence of porphyrin-based magnetic nanocatalysts (Table 7). Appropriate reaction time and the use of green oxidant like H_2O_2 for epoxidation in the mild condition are the considerable advantages of this research compared to some other previously reported data.

Table 7. Oxidation of cyclooctene in the presence of porphyrin-based magnetic nanocatalysts at room temperature.

No.	Catalyst	Oxidant	Time (h)	Conversion %	Ref.
1	Fe_3O_4@*n*SiO_2–NH_2-MnPor	TBAO	20	97	43
2	Fe_3O_4@SiO_2-N_3@[MnTHPP]	TBHP	12	85	53
3 [a]	Mn(TPP)OAc@SMNP	TBHP	4.5	98	6
4	Fe3O4@*n*SiO_2@MCM-41-MnP	PhIO	6	77	54
5	FeP2-S2-Mag	PhIO	1	88	55
6	Mn(TPP)Cl@ImeSiO$_2$@Fe_3O_4	$NaIO_4$	3	98	18
7	[Mn(TPP)Cl@ImeSiO$_2$@Fe_3O_4]	H_2O_2	3	36	18
8	Fe_3O_4/SiO_2/NH_2-Mn(TCPP)OAc	H_2O_2	5	87	This work
9 [a]	Fe_3O_4/SiO_2/NH_2-Fe(TCPP)Cl	H_2O_2	5	97	This work

[a]Higher Temperature was necessary

Conclusion

In summary, the present study proposed a simple and practical method for preparation of effective nanocatalysts for the oxidation of organic substrates. Mn(TCPP)OAc and Fe(TCPP)Cl were immobilized on the surface of amine functionalized silica-coated magnetic nanoparticles via covalent bond to produce the magnetically separable nanocatalysts. The prepared nanoparticles were fully characterized and applied as efficient nanocatalysts for the oxidation of olefins with H_2O_2 and the catalytic activity of Fe_3O_4/SiO_2/NH_2-Mn(TCPP)OAc and Fe_3O_4/SiO_2/NH_2-Fe(TCPP)Cl were compared in the same condition. The obtained results reveal higher efficiency of Mn-catalyst compared to the Fe-catalyst and the results were demonstrated that the catalytic activity and stability of metalloporphyrins are greatly improved by immobilization onto the surface of magnetic nanoparticles. The obtained AAS data and the XRD pattern of the used catalyst proved high stability of magnetic nanoparticles under the oxidation reaction even in the presence of excess amount of the oxidant. The ease of separation by an external magnet and reusability of the catalyst for at least five runs without significant leaching or decreasing the catalytic activity were merits of the prepared nanocatalysts.

Acknowledgements

This work was supported by K.N. Toosi University of Technology research council and Iran National Science Foundation (INSF) [grant No. 98026139].

References

1 K. Bauer, D. Garbe, H. Surburg, Common Fragrance and Flavor Materials Wiley-VCH, New York, 1997.

2 M. Beller, C. Bolm, Transition Metals for Fine Chemicals and Organic Synthesis; vol. 2, Wiley, 1998.

3 T. Mallat, A. Baiker, *Chem. Rev.*, 2004, **104** (6), 3037-3058.

4 S. Rayati, F. Nejabat, F. Panjiali, *Catal. Commun.*, 2019, **122**, 52-57.

5 A. Zarrinjahan, M. Moghadam, V. Mirkhani, S. Tangestaninejad, I. Mohammadpoor-Baltork, *J. Iran. Chem. Soc.*, 2016, **13**, 1509-1516.

6 A. Rezaeifard, P. Farshid, M. Jafarpour, G.K. Moghaddam, *RSC Adv.*, 2014, **9**, 9189–9196.

7 A. Maleki, *Ultrason. Sonochem.*, 2018, **40**, 460-464.

8 A. Mukherjee (Eds.), Biomimetic Based Applications; In Tech, Croatia, 2011.

9 M. Sono, M. P. Roach, E. D. Coulter, J. H. Dawson, *Chem. Rev.*, 1996, **96 (7)**, 2841-2887.

10 B. Meunier, Biomimetic oxidations catalyzed by transition metal complexes; Imperia College Press, 2000.

11 R.V. Eldik, J. Reedijk, Homogeneous biomimetic oxidation catalysis; Academic Press, 2006.

12 S. Masoudian, H. Yahyaei, *Indian J. Chem.*, 2011, **50**, 1002-1005.

13 J. Yoo, N. Park, J.H. Park, S. Kang, S. M. Lee, H.J. Kim, H. Jo, J.G. Park, S.U. Son, *ACS Catal.*, 2015, **5** (1), 350-355.

14 X-F. Huangk, G-P. Yuan, G. Huang, S-J. Wei, *J. Ind. Eng. Chem.*, 2019, **77**, 135-145.

15 A. Heidarnezhad, F. Zamani, *Catal. Commun.*, 2015, **60**, 105-109.

16 J. Li, H. Gao, L. Tan, Y. Luan, M. Yang, *Eur. J. Inorg. Chem.*, 2016, **30**, 4906-4912.

17 H.R. Mardani, M. Ziari, *Res. Chem. Intermed.*, 2018, **44** (11), 6605-6619.

18 M.S. Saeedi, S. Tangestaninejad, M. Moghadam, V. Mirkhani, I. Mohammadpoor-Baltork, A.R. Khosropour, *Mater. Chem. Phys.*, 2014, **146**, 113-120.

19 H. Ghafuri, S. Rahmani, R. Rahimi, E. Mohammadiyan, *RSC Adv.*, 2016, **6**, 62916-62922.

20 K. Zhang, J.M. Suh, T.H. Lee, J.H. Cha, J. Choi, H.W. Jang, R.S. Varma, M. Shokouhimehr, Nano Convergence, 2019, **6** (1), 1-7.

21 S. Rayati, S. Rezaei, F. Nejabat, *J. Cooed. Chem.*, 2019, **72**, 1466-1479.

22 H. Sharghi, M.H. Beyzavi, A. Safavi, M.M. Doroodmand, R. Khalifeh, *Adv. Synth. Catal.*, 2009, **351**, 2391 – 2410.

23 M.E. Lipin´ska, S.L.H. Rebelo, C. Freire, *J. Mater. Sci.*, 2014, **9**, 1494–1505.

24 F. Nejabat, S. Rayati, *J. Ind. Eng. Chem.*, 2019, **69**, 324-330.

25 A. Rezaeifard, M. Jafarpour, P. Farshid, A. Naeimi, *Eur. J. Inorg. Chem.*, 2012, **33**, 5515-5524.

26 Z. Feng, Y. Xie, F. Hao, P. Liu, H. Luo, *J. Mol. Catal. A: Chem.*, 2015, **410**, 221–225.

27 K. Hayashi, S. Wataru, T. Yogo, *J. Asian Ceram. Soc.*, 2014, **2**, 429–434.

28 L. Sun, Y. Li, M. Sun, H. Wang, S. Xu, C. Zhang, Q. Yang, *New J. Chem.*, 2011, **35**, 2697–2704.

29 Q. Zhang, H. Su, J. Luo, Y. Wei, *Green Chem.*, 2012, **14**, 201-208.

30 C.A. Henriques, A. Fernandes, L.M. Rossi, M.F. Ribeiro, M.J.F. Calvete, M.M. Pereira, *Adv. Funct. Mater.*, 2016, **26** (19), 3359–3368.

31 A. Maleki, R. Rahimi, S. Maleki, *Environ. Chem. Lett.*, 2016, **14**, 195-199.

32 W. Cai, M. Cai, X. Weng, W. Zhang, Z. Chen, *Mat. Sci. Eng. C,* 2019**, 98**, 65–73.

33 A. Isogai, L. Bergström, *Curr. Opin. Green Sustain. Chem.*, 2018, **12**, 15-21.

34 E.N. Kolobova, A.N. Pestryakov, N. Bogdanchikova, V. C. Corberán, *Catal. Today*, 2019, **333**, 81-88.

35 M.F. McLaughlin, E. Massolo, T.A. Cope, J.S. Johnson, *Org. Lett.*, 2019, **21** (16), 6504-6507.

36 H. Su, C. Yu, Y. Zhou, L. Gong, Q. Li, P.J.J. Alvarez, M. Long, *Water Res.*, 2018, **140**, 354-363.

37 A. Paradisi, E.M. Johnston, M. Tovborg, C.R. Nicoll, L. Ciano, A. Dowle, J. McMaster, Y. Hancock, G.J. Davies, P.H. Walton, *J. Am. Chem. Soc.,* 2019, **46**, 18585-18599.

38 A.D. Adler, F.R. Longo, W. Shergalis, *J. Am. Chem. Soc.*, 1964, **86**, 3145-3149.

39 J.W. Buchler, G. Eikellmann, J. Puppe, K. Rohback, H. Schneehage, D. Weck, *Justus. Liebigs. Ann. Chem.*, 1971, **745** (1), 135-151.

40 P. Battioni, J.F. Bartoli, D. Mansuy, Y.S. Byunand, T.G. Traylor, *J. Chem. Soc., Chem. Commun.*, 1992, **15**,1051-1053.

41 X.Q. Liu, Z.Y. Ma, J.M. Xing, H.Z. Liu, *J. Magn. Mater.*, 2004, **270**, 1-6.

42 F. Wypych, A. Bail, M. Halma, S. Nakagaki, *J. Catal.*, 2005, **234** (2), 431-437.

43 M. Bagherzade, A. Mortazavi-Manesh, *RSC Adv.*, 2016, **6** (47), 41551-41560.

44 A. Arabanian, M. Mohammadnejad, S. Balalaie, *J. Iran. Chem. Soc.*, 2010, **7**, 840-845.

45 S. Li, S.R. Zhai, Q.D. An, M.H. Li, Y. Song, X.W. Song, *Mater. Res. Bull.*, 2014, **60**, 665–673.

46 S. Bakhshayesh, H. Dehghani, *Mater. Res. Bull,* 2013, **48** (7), 2614–2624.

47 J.P. Mbakidi, F. Brégier, T.S. Ouk, R. Granet, S. Alves. E. Rivière, S. Chevreux. G. Lemercier, V. Sol, *chempluschem*, 2015, **80**, 1416-1426.

48 F. Mohammadi, A. Esrafili, M. Kermani, M. Behbahani, *J. Iran. Chem. Soc.*, 2018, **15**, 421–429.

49 Y. Wang, P. Jiang, W. Zhang, J. Zheng, *Appl. Surf. Sci.*, 2013, **270**, 531– 538.

50 C.A. Henriques, A. Fernandes, L.M. Rossi, M.F. Ribeiro, M.J.F. Calvete, M.M. Pereira, *Adv. Funct. Mater.*, 2016, **26**, 3359-3368.

51 N. Iranpoor, D. Mohajer, A. R. Rezaeifard, *Tetrahedron Lett.*, 2004, **45**, 3811-3815.

52 D. Mohajer, G. Karimipour, M. Bagherzadeh, *New J. Chem.*, 2004, **28**, 740 -747.

53 M. Bagherzadeh, A. Mortazavi-Manesh, M. Hosseini, *Inorg. Chem. Commun.*, 2019, **107**, 107495.

54 F.B. Zanardi, I.A. Barbosa, P.C. de Sousa Filho, L.D. Zanatta, D.L. da Silva, O.A. Serra, Y. Iamamoto, *Micropor. Mesopor. Mat.*, 2016, **219**, 161 -171.

55 G.M. Ucoski, F.S. Nunes, G.D.-Silva, Y.M. Idemori, S. Nakagaki, *Appl. Catal. A Gen.*, 2013, **459**, 121– 130.

View Article Online
DOI: 10.1039/D0NJ04190D

56 A. Farokhi, M.Hosseini-Monfared, *NewJ. Chem.* 2016, **40**, 5032-5035.

View Article Online
DOI: 10.1039/D0NJ04190D

A simple method for the functionalization of magnetic nanoparticles, which produced by the attachment of metalloporphyrin onto the surface of amine functionalized silica-coated magnetic nanoparticles via amide bond.